SAND2012-6283C

Microstructural analysis of reconsolidated crushed salt at 250°C, under hydrostatic and shear stresses

Rachel Wells[1,2], Steve Bauer[2], Frank Hansen[2], Scott Broome[2], Alex Urquhart[2]

[1] Texas A&M University (Ph.D. in Geology, Expected Graduation Date Spring 2014),

[2] Sandia National Laboratories/NM, U.S. Department of Energy

August 2, 2012

Introduction

Bedded salt formations are being considered as possible locations for a nuclear waste repository because salt is impermeable and has the unique ability to flow and reconsolidate, allowing the nuclear waste to be completely sealed (Brodsky et al., 1996). The Waste Isolation Pilot Plant (WIPP), southeastern New Mexico, is an active research and development facility using bedded salt to store nuclear waste. Previous studies (Callahan, 1999) have investigated the mechanical properties of crushed salt (i.e. the mined material used to cover the waste) at room temperature, where water is expected to influence deformation.

Question – What deformation mechanisms are active during salt reconsolidation at high temperature conditions, when free water (i.e. pore fluid) is expected to be driven out?

Goal – The purpose of this study is to determine the deformation mechanisms of WIPP salt at 250 °C. We show, under experimentally deformed conditions, WIPP salt first deforms by brittle failure, followed by a combination of diffusion mass transfer (i.e. pressure solution) and dislocation creep.

Methods - Samples were dried at 105 °C for several days then experimentally deformed at 250 °C in a triaxial apparatus under hydrostatic-quasistatic, shear-quasistatic, and creep conditions. Deformation mechanisms are inferred from microstructural observations made using optical and electron microscopy. Both secondary electron images (SE) and backscatter electron images (BSE) were collected on a scanning electron microscope. Porosity is determined by a random point count of grain and pore space.

Microstructural Observations of Deformed Salt

Hydrostatic-Quasistatic

(Confining Pressure 20 MPa; Differential Stress 0 MPa)

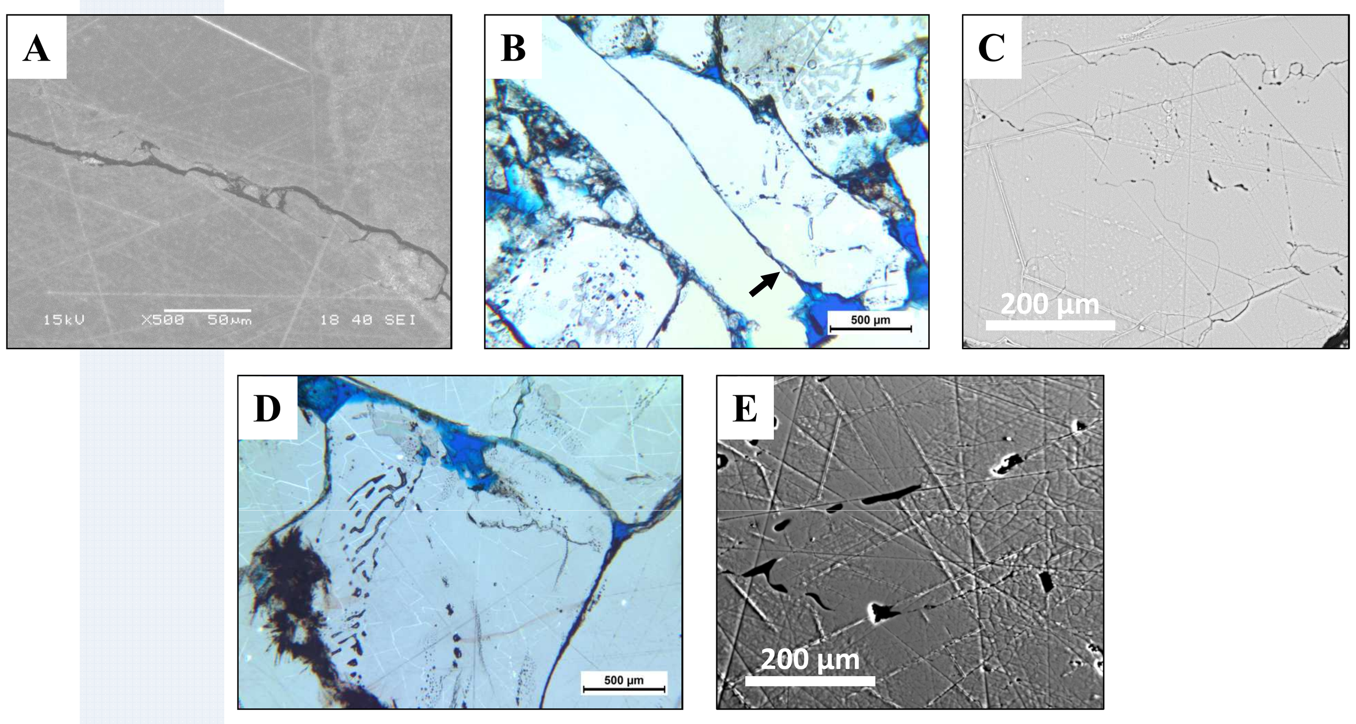

Figure 1. A) Fine grains (20-75 µm) with faint grain boundaries are observed at coarser grain boundaries. SE image. B) Elongated, folded grains are common. Note the fine (<50 µm), lenticular grains between the coarser grains (arrow). Photomicrograph. C) Fractures connecting small inclusions occur in a coarse grain. Note the "floating" grain in the bottom-left corner. BSE image. D) Island-channel inclusions are common. Photomicrograph. E) Irregular shaped inclusions appear to outline a grain, but a grain boundary is not observed. SE image.

Porosity ranges from 10.0-13.6%, with a mean of 12.4%.

Shear-Quasistatic

(Confining Pressure 10 MPa; Differential Stress ~6.4 MPa)

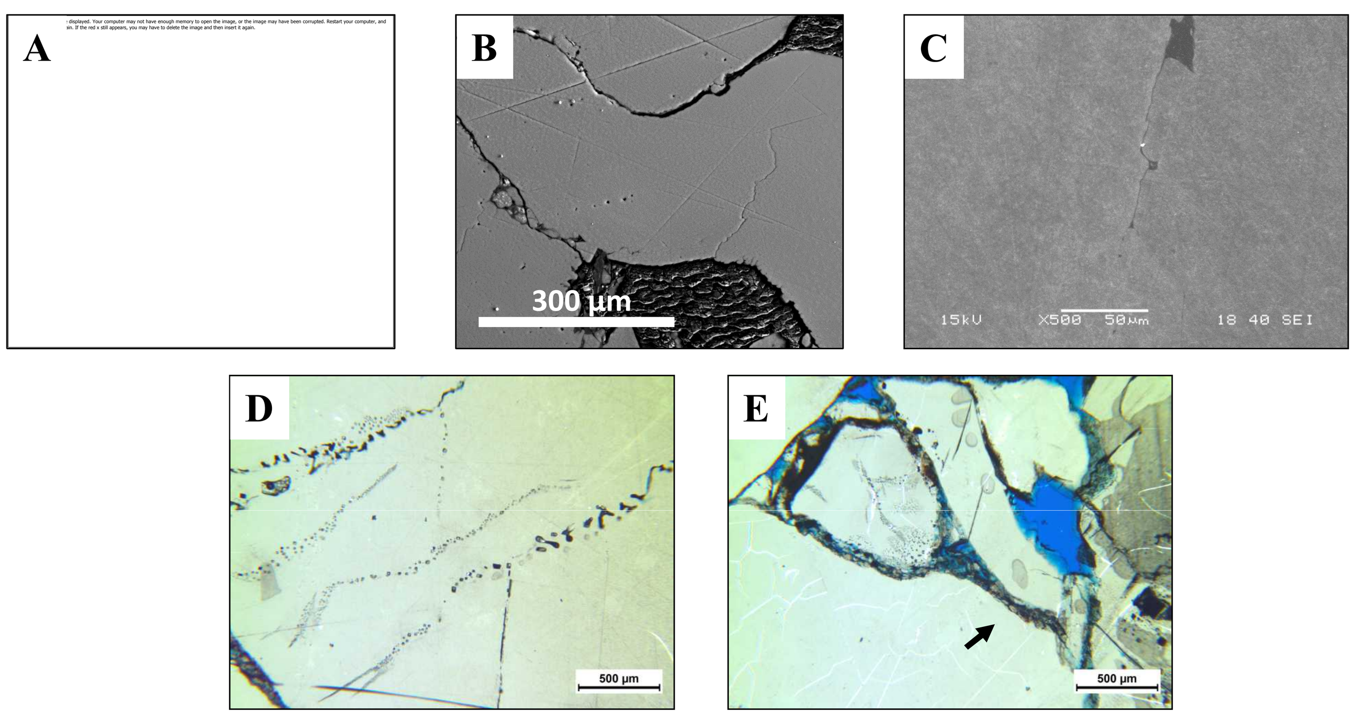

Figure 2. A) An irregular-interpenetrating grain boundary occurs between two coarse (>0.5 mm) grains. SE image. B) A folded grain, with inclusions (black dots) and fractures, is observed between two coarser grains. SE image. C) Fine grains (20-100 µm) with faint grain boundaries are observed between coarser grains. SE image. D) Island-channel shaped inclusions compared to square shaped inclusions. Photomicrograph. E) Lenticular, fine grains commonly occur along coarser grain boundaries (arrow). Photomicrograph.

Porosity ranges from 8.8-10.4%, with a mean of 9.8%.

Shear-Quasistatic

(Confining Pressure 10 MPa; Differential Stress ~11 MPa)

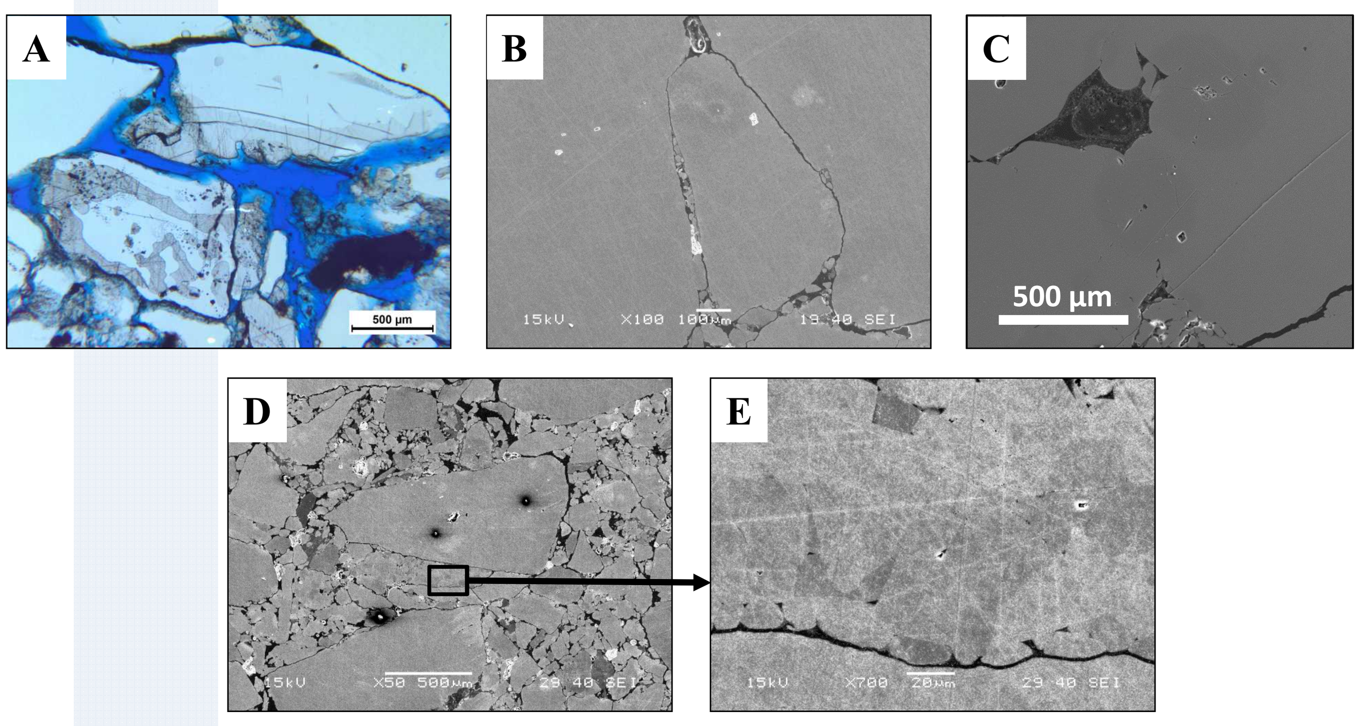

Figure 3. A) Irregular grain boundaries are common in coarser (>0.2 mm) grains. Photomicrograph. B) Aligned, lenticular grains (20-100 µm) are observed at coarser grain boundaries. Photomicrograph. C) Scalloped shaped grain boundary with irregular (non-square) shaped inclusions. SE image. D) Variation in grain size is common. SE image. E) The grain (or possibly a clast) appears to be composed of finer (20-50 µm) grains, but their grain boundaries are indiscernible. SE image.

Porosity ranges from 9.6-12.0%, with a mean of 11.1%.

Creep

(Confining Pressure 2.5 MPa; Differential Stress 5 MPa)

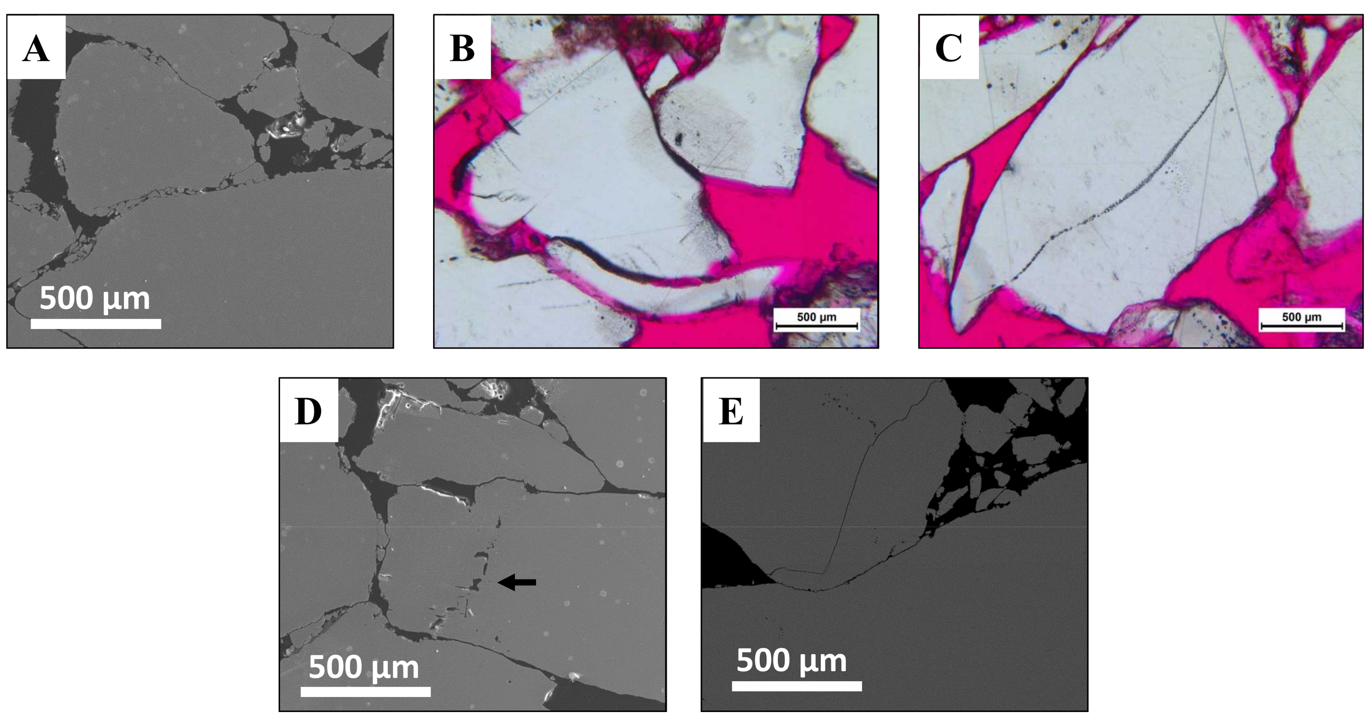

Figure 4. A) Fine (<100 µm) grains between coarser grain boundaries are not very common. SE image. B) An elongated grain is folded between two coarser grains. Photomicrograph. C) Trail of inclusions originate from a right-angle along the grain boundary. Note that the trail of inclusions is curved (typically straight). Photomicrograph. D) Several channel shaped inclusion (arrow) appear to separate two grains. SE image. E) Interpenetrating grain boundaries are observed but are not common within this sample.

Porosity ranges from 19.2-25.6%, with a mean of 22.4%.

Deformation Mechanisms

Microstructure Summary	HQ-250-02	SQ-250-01	SQ-250-02	CR-250-01
Intragranular fractures				
Fine grains at grain boundaries				
Folded grains				
Irregular shaped inclusions				
Non-linear trail of inclusions				
Irregular grain boundaries				
Interpenetrating grain boundaries				
Fine-grain clasts				
Mean porosity	12.4	11.1	9.8	22.4

present common

1. **Brittle Deformation** – All of the samples contain fractures and offset fractures suggesting brittle failure. The fractures are most likely occurring early in the deformation (during loading) because no fractures cross-cut folded grains or grains with irregular boundaries.
2. **Diffusive Deformation** – Interpenetrating and irregular grain boundaries are evidence for diffusive mass transfer.
   A. Fluids typically assist diffusion, but the samples were dried to insure no free fluids were present. Trapped fluids (inclusions) are common and these inclusions could have been freed by fracturing during heating, allowing fluids to influence deformation.
   B. If salt is being dissolved and transported, forming stylolites, the material should be precipitated somewhere else in the sample, which has not been observed to date. This is not to say that diffusion between two halite grains is not occurring, commonly resulting in in interpenetrating grain boundaries.
3. **Dislocation Creep** – Dislocation creep is possible at these conditions, which could be leading to the formation of the folded grains; however, more evidence (i.e. etching for dislocations) is needed to demonstrate if dislocation creep is active.

Conclusions

1. Salt will deform by fracturing, followed by diffusion mass transfer and possibly dislocation creep at 250 °C.
2. Diffusion mass transfer is active during deformation at 250 °C, due in part, to the release of trapped fluids.
3. Fluids are being released because of fracturing, either during loading or because the salt crystal are being heated. If the material in the inclusion (e.g. brine) is heated, the fluid and/or gas will expand, resulting in a fracture. It is not clear if dislocation creep is active during deformation. Etching of the dislocations, if present, is needed to determine dislocation creep is leading to the fine-grained halite or the folding of the coarser, elongated halite grains.

References

Brodsky, N.S., Hansen, F.D., and Pfeifle, T.W., 1996. Properties of dynamically compacted WIPP salt: Fourth Conference on the Mechanical Behavior of Salt, State College, Pennsylvania

Callahan, C.D., 1999. Crushed Salt Constitutive Model, Sand98-2680. Albuquerque, NM, Sandia National Laboratories